High quality $Fe_{3-\delta}O_4$/InAs hybrid structure for electrical spin injection

Marhoun Ferhat[a)]
CREST-JST, Kawaguchi, Saitama 332-0012, Japan

Kanji Yoh
CREST-JST, Kawaguchi, Saitama 332-0012, Japan and Research Center for Integrated Quantum Electronics, Hokkaido University, Sapporo, 060-8628, Japan

(Received 21 October 2006; accepted 10 February 2007; published online 14 March 2007)

Single crystalline $Fe_{3-\delta}O_4$ ($0 \leqslant \delta \leqslant 0.33$) films have been epitaxially grown on InAs (001) substrates by molecular beam epitaxy using O_2 as source of active oxygen. Under optimum growth conditions, *in situ* real time reflection high-energy electron diffraction patterns, along with *ex situ* atomic force microscopy, indicate that (001) $Fe_{3-\delta}O_4$ can be grown under step-flow-growth mode with a characteristic $(\sqrt{2}\times\sqrt{2})R45$ surface reconstruction. X-ray photoelectron spectroscopy demonstrates the possibility of obtaining iron oxides with compositions ranging from Fe_3O_4 to γ-Fe_2O_3. Measurements with a superconducting quantum interference device magnetometer at 300 K show good magnetic properties, suggesting that iron-based oxides may be promising for spintronic applications. © *2007 American Institute of Physics*. [DOI: 10.1063/1.2713784]

During the last decade, there has been a considerable increase of studies on hybrid structures combining both semiconductors and magnetic materials. These studies are motivated by possible applications in the nascent field of spintronics, since the electron spin degree of freedom in hybrid structures is believed to be a source of a rich array of new physical phenomena. Different approaches have been adopted for the selection of adequate spin injectors including ferromagnetic metals,[1,2] dilute magnetic semiconductors,[3] and Heusler alloys.[4] The use of magnetic semiconductors in this field presents the formidable task of increasing the Curie temperature. Ferromagnetic metal and Heusler alloys on the other hand suffer from structural and interfacial problems during their growth. Quite surprisingly, there are few reports on iron oxide based half metals, which exhibit a large polarization at the Fermi level making them very attractive for spin injection into semiconductors.

Fe_3O_4 or magnetite belongs to a large family of iron-based oxides commonly called ferrites. Our choice for this material as a possible efficient spin injector into semiconductors stems from its physical properties, which are attractive in many respects. (i) It has half metallic character with a large spin polarization at the Fermi level.[5,6] (ii) It possesses an electrical resistivity of the same order of magnitude as a semiconductor, making the conductivity mismatch problem less severe than in the case of metals. (iii) It has a Curie temperature of about 850 K, well above room temperature. This study will combine the use of magnetite with InAs substrates. InAs is used because of high room temperature electron mobility and, more importantly, because of its large and tunable spin-orbit coupling strength (small ratio between the Rashba and Dresselhauss terms), important for spin-based devices.[7] Although the growth of iron oxides on metallic and oxide based substrates is a very well documented subject,[8] there are only few reports on the growth of iron oxides on semiconducting substrates.

The purpose of the present letter is to extend the only work available[9] on the growth of Fe_3O_4 on InAs with special emphasis on the growth mechanism and crystal quality using molecular beam epitaxy (MBE) technique. Combining real time *in situ* reflection high-energy electron diffraction (RHEED) and *ex situ* atomic force microscopy (AFM), we demonstrate the possibility of obtaining high quality Fe_3O_4 (001) with good magnetic properties.

Epiready *p*-doped InAs (001) wafers were used as received. The samples, with a typical size of about $7\times10\text{mm}^2$, were loaded in the solid source MBE system, and the oxide layer was removed by annealing at around 510 °C under an As_4 pressure of 1×10^{-5} Torr. A 500-nm-thick InAs buffer layer was grown at 450 °C using a beam-equivalent-pressure ratio of As_4 to In of about 12. This ensured the growth of a high quality InAs buffer layer, exhibiting a sharp and well ordered (2×4) surface structures termination.

Immediately after this, the samples were transferred through an ultrahigh vacuum module to an attached MBE chamber dedicated to the growth of iron oxides. The oxide MBE chamber is equipped with three metal beam sources, where contactless Fe rods were used to insure minimum contamination. The chamber was modified to include a high purity molecular oxygen reservoir with a precise variable leak valve for the control of the oxygen partial pressure. An optimum growth temperature of 300 °C with oxygen partial pressures of 7.5×10^{-7} and 4×10^{-6} Torr was found to yield Fe_3O_4 and γ-Fe_2O_3, respectively. The calibration of the growth temperature was performed by carefully monitoring the $(2\times4)\rightarrow(4\times2)$ InAs surface structure transition (at about 410 °C) as well as the melting point of In (157 °C). In all cases the growth rate was fixed to ~10 nm/h.

The RHEED patterns of the InAs (001) along the [110] and [−110] azimuths together with those of 20-nm-thick Fe_3O_4 along the [110] and [100] azimuths of InAs (001) are shown in Fig. 1. The RHEED patterns [Figs. 1(c) and 1(d)] are similar to those observed[10,11] in epitaxial Fe_3O_4/MgO (001) but rotated by 45° relative to the [100] azimuth of InAs (001). The epitaxial relationship is therefore [110] Fe_3O_4 (001)//[100] InAs (001) with a clear $(\sqrt{2}\times\sqrt{2})R45$ surface structure.

[a)]Electronic mail: ferhat@eng.hokudai.ac.jp

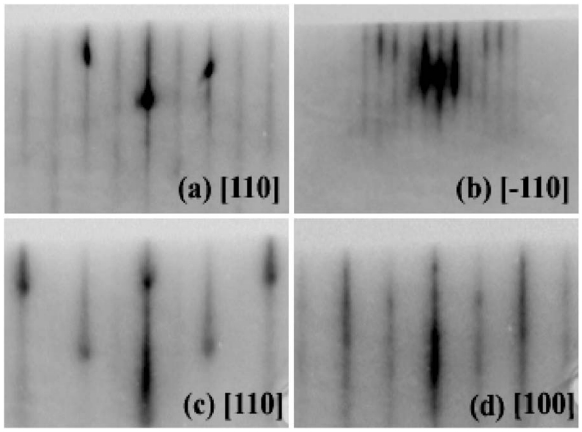

FIG. 1. RHEED patterns for bare (001) InAs along (a) the ⟨110⟩ and (b) ⟨−110⟩ just before the growth and for 20-nm-thick Fe_3O_4 along (c) the ⟨110⟩ and (d) the ⟨100⟩ azimuths. All azimuths are refereed to the InAs substrate.

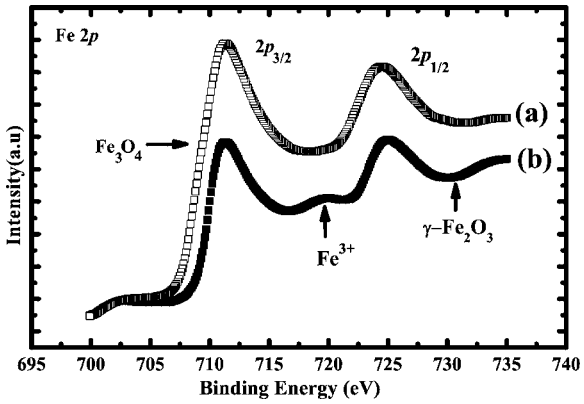

FIG. 3. Fe 2*p* high-resolution XPS spectra for 20-nm-thick $Fe_{3-\delta}O_4$/InAs grown at 300 °C under oxygen partial pressures of (a) 7.5×10^{-7} Torr and (b) 4×10^{-6} Torr. The compositions obtained are indicated in the figure.

The lattice constant along [110] was found to be the same as that of InAs ($a_{[110]}$=8.57 Å), indicating the full pseudomorphic nature of the films. This explains the 45° rotation of Fe_3O_4 ($a_{[100]}$=8.40 Å) relative to bare InAs, where the lattice mismatch is reduced to only 1.9%. A similar situation was recently encountered in Fe_3O_4/GaAs,[12] although the large lattice mismatch of 5% probably leads to films of quality inferior to the present case. However, even a lattice mismatch of 1.9% is not expected to yield the sharp and streaky patterns we observe in Figs. 1(c) and 1(d). This is because such a highly tensile strain should induce three-dimensional growth mode, which is manifested by spots in the RHEED patterns.

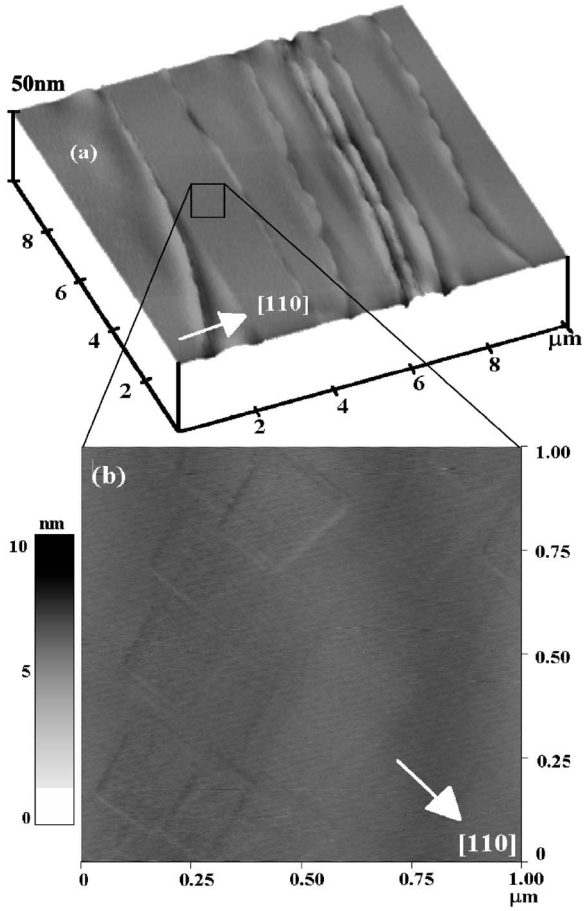

FIG. 2. Typical AFM images of 20-nm-thick Fe_3O_4/InAs. (a) Topography showing a stepped surface with large terraces. (b) Enhanced view of a terrace showing rectangular features attributed to domains with different surface terminations.

Figure 2(a) shows the AFM topography of an as-grown Fe_3O_4 film with macroscopic step edges (up to 10 nm in height) separated by flat terraces (up to 2 μm wide) running along the [−110] direction of the InAs substrate. Close inspection of the terraces shows them to be atomically flat with rectangular features [Fig. 2(b)], probably reflecting domains with different surface terminations.[13] Both our AFM images together with the absence of RHEED oscillations during the growth are strong evidence of a step-flow-growth mode in the present case. In order to explain the occurrence of this particular growth mode, recall that in contrast to GaAs (001), the $(2\times4)\rightarrow(4\times2)$ phase transition in InAs (001) is first order owing to the strong lateral interaction of the As-surface unit in the (2×4) structure of InAs (001).[14,15] Consequently, the As-rich surface structure is well ordered and highly uniform.

This is particularly true in our case, as can be clearly seen in the RHEED patterns of InAs [Figs. 1(a) and 1(b)] just before the growth. The large size of our sample holder, however, required about 30 min to stabilize the substrate temperature. This relatively prolonged annealing at 300 °C leads to preferential As desorption with the creation of monomolecular steps running along the [−110] (direction of the As dimer rows), as in the case of Ref. 15, and is the origin of the step-flow-growth mode observed. However, the steps height in Fig. 2(a) is not monomolecular, and some terraces are over 1 μm wide, evidence of a step-bunching instability. Two mechanisms are qualitatively relevant to our experimental results. The first mechanism proposed by Tersoff *et al.*[16] has its origin in the large elastic strain of our pseudomorphic films (1.9% mismatch). The elastic strain relaxation at steps produces a long-range attractive interaction between steps and therefore step bunching. The second mechanism proposed by Kandel and Weeks[17] is related to the surface reconstruction. The presence of differently reconstructed areas on the terraces might impede the motion of steps, thus decreasing their velocity and leading to step bunching. The rectangular features observed in Fig. 2(b) very likely represent areas with different surface terminations thus kinetically leading to a step-bunching instability. The existence of some terraces extending up to about 2 μm wide suggests the com-

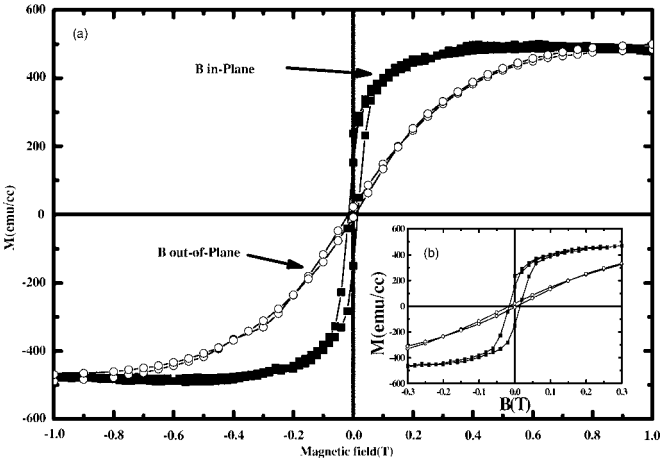

FIG. 4. (a) Room temperature hysteresis loop obtained with a superconducting quantum interference device magnetometer for 20-nm-thick Fe_3O_4/InAs with a magnetic field applied along both the parallel and perpendicular directions with respect to the film plane. (b) Enlarged view of the hysteresis loops.

bined action of both strain and surface reconstruction mechanisms during the growth.

Although Fe_3O_4 has a rather similar crystal structure to that of γ-Fe_2O_3 in typical x-ray photoelectron spectroscopy (XPS) measurements, a distinctive satellite structure due to charge transfer screening appears in the Fe $2p$ core level spectrum of γ-Fe_2O_3 but not in that of magnetite. Figures 3(a) and 3(b) shows the high-resolution Fe $2p$ XPS spectra (Mg$K\alpha$) of 20-nm-thick iron oxide films grown at the same substrate temperature of 300 °C but under O_2 partial pressures of 7.5×10^{-7} and 4×10^{-6} Torr, respectively. All binding energies were corrected for charging effects by setting the O $1s$ at 530.1 eV. Clearly, Fig. 3(b) exhibits a "shake-up" satellite at about 719.7 eV, which is characteristic of Fe^{3+} ions, thus indicating the formation of γ-Fe_2O_3. Since Fe_3O_4 contains both Fe^{2+} and Fe^{3+} ions, their mutual contribution to the Fe $2p$ XPS spectra between the main spin-orbital peaks (Fe $2p_{1/2}$ and Fe $2p_{3/2}$) gives rise to a vanishing and unresolved component. The absence of the shake-up satellite in Fig. 3(a) can be considered as evidence of near stoichiometric Fe_3O_4. This is not unexpected since a large O_2 partial pressure was required to obtain γ-Fe_2O_3, which can be considered as an oxidized form of Fe_3O_4. Strictly speaking, the growth of Fe_3O_4 yields in general a nonstoichiometric magnetite, which should be written as $Fe_{3-\delta}O_4$ with $\delta=0$ for pure magnetite and $\delta=0.33$ for maghemite or γ-Fe_2O_3. Quantification of the vacancy parameter δ is quite challenging, but a close comparison of the shape of the XPS spectra in Ref. 18 (Fig. 9) with those depicted in Fig. 3 indicates that the deviation from stoichiometry, if present, is likely to be very small in our films.

Figure 4 shows the hysteresis loops measured at 300 K for the optimized Fe_3O_4 film. It exhibits an easy in-plane magnetization [Fig. 4(a)] due to the shape anisotropy with a coercive field of about 0.022 T and a saturation magnetization of about 483 emu/cc, in close agreement with the value reported for bulk magnetite.[19] The in-plane saturation was achieved at a field of about 0.5 T, whereas a field of about 1 T was necessary for the out-of-plane direction. This is in contrast with the previous results,[20,21] where the presence of antiphase boundaries (APBs) leads to unsaturated magnetization at fields as large as 7 T. A plausible explanation of this difference should be sought in the growth mechanism. In a typical two-dimensional layer-by-layer mode, the coalescence of islands during the growth is likely to form APBs extending along all the film thicknesses.[22] In the step-flow-growth mode, however, the nucleation occurs preferentially at the step edges, and the growth extends laterally leading to a reduced APB density. Perhaps the present situation is similar to the case of GaAs on Ge,[23] where APB-free films were obtained by appropriate surface treatment.

In summary, high quality (001) $Fe_{3-\delta}O_4$ films were epitaxially grown on a (001) InAs substrate using molecular beam epitaxy. The Fe $2p$ XPS core level spectra demonstrate the possibility of growing in a controlled manner both Fe_3O_4 and γ-Fe_2O_3 with small deviations from stoichiometry. The magnetic properties of the films show a bulklike behavior that can be tentatively explained by reduced APBs owing to the step-flow-growth mode observed. The overall results lend credibility to the promise of iron-based oxides for spintronic applications.

The authors are grateful to O. B. Wright, A. Subagyo, K. Sueoka, and Y. Suda for useful discussions. This work was partially supported by the Japanese Ministry of Education, Culture, Sports, Science and Technology.

[1] G. A. Prinz, *Ultra Thin Magnetic Structures II* (Springer, Berlin, 1994), Vol. II, p. 1.
[2] K. Yoh, H. Ohno, Y. Katano, K. Sueoka, K. Mukasa, and M. E. Ramsteiner, Semicond. Sci. Technol. **19**, S386 (2004).
[3] R. Fiederling, M. Keim, G. Reuscher, W. Ossau, G. Schmidt and A. Waag, Nature (London) **402**, 787 (1999), Y. Ohno, D. K. Young, B. Beschoten, F. Matsukura, and H. Ohno, *ibid.* **402**, 790 (1999).
[4] C. J. Palmstrøm, MRS Bull. **28**, 725 (2003).
[5] Yu. S. Dedkov, U. Rüdiger, and G. Güntherodt, Phys. Rev. B **65**, 064417 (2002).
[6] J. J. Versluijs, M. A. Bari, and J. M. D. Coey, Phys. Rev. Lett. **87**, 026601 (2001).
[7] K. Yoh, M. Ferhat, A. Riposan, and J. M. Millunchick, AIP Conf. Proc. **772**, 1315 (2005).
[8] S. A. Chambers, Surf. Sci. Rep. **39**, 105 (2000).
[9] E. J. Preisler, J. Brooke, N. C. Oldham, and T. C. McGill, J. Vac. Sci. Technol. B **21**, 1745 (2003).
[10] J. F. Bobo, D. Basso, E. Snoeck, C. Gatel, D. Hrabovsky, J. L. Gauffier, L. Ressier, R. Mamy, S. Visnovsky, J. Hamrle, J. Teillet, and A.. R. Fert, Eur. Phys. J. B **24**, 43 (2001).
[11] Y. Gao and S. A. Chambers, J. Cryst. Growth **174**, 446 (1997).
[12] Y. X. Lu, J. S. Claydon, Y. B. Xu, S. M. Thompson, K. Wilson, and G. Van der Laan, Phys. Rev. B **70**, 233304 (2004).
[13] S. F. Ceballos, G. Mariotto, K. Jordan, S. Murphy, C. Seoighe, and I. V. Shvets, Surf. Sci. **548**, 106 (2004).
[14] H. Yamaguchi and Y. Horikoshi, Phys. Rev. Lett. **70**, 1299 (1993).
[15] H. Yamaguchi and Y. Horikoshi, Phys. Rev. B **48**, 2807 (1993).
[16] J. Tersoff, Y. H. Phang, Z. Zhang, and M. G. Lagally, Phys. Rev. Lett. **75**, 2730 (1993).
[17] D. Kandel and J. D. Weeks, Phys. Rev. B **49**, 5554 (1994).
[18] T. Fuji, F. M. F. de Groot, G. A. Sawatzky, F. C. Voogt, T. Hibma, and K. Okada, Phys. Rev. B **59**, 3195 (1999).
[19] Z. Kakol and J. M. Honig, Phys. Rev. B **40**, 9090 (1989).
[20] D. T. Margulies, F. T. Parker, M. L. Rudee, F. E. Spada, J. N. Chapman, P. R. Aitchison, and A. E. Berkowitz, Phys. Rev. Lett. **79**, 5162 (1997).
[21] W. Eerenstein, T. T. M. Palstra, T. Hibma, and S. Celotto, Phys. Rev. B **66**, 201101(R) (2002).
[22] W. Hong, H. N. Lee, M. Yoon, H. M. Christen, D. H. Lowndes, Z. Suo, and Z. Zhang, Phys. Rev. Lett. **95**, 095501 (2005).
[23] S. M. Ting and E. A. Fitzgerald, J. Appl. Phys. **87**, 2618 (2000).